Interaction of C-Terminal Loop 13 of Sodium-Glucose Cotransporter SGLT1 with Lipid Bilayers†

M. Mobeen Raja and Rolf K. H. Kinne*

Department of Epithelial Cell Physiology, Max Planck Institute of Molecular Physiology, Otto-Hahn-Strasse 11, 44227 Dortmund, Germany

Received February 21, 2005; Revised Manuscript Received May 2, 2005

ABSTRACT: We have previously shown that C-terminal loop 13 of SGLT1 acts as a major binding domain for the aglucon residues of D-glucose transport inhibitors, phlorizin (Raja, M. M., Tyagi, N. K., and Kinne, R. K. H. (2003) Phlorizin Recognition in a C-terminal Fragment of SGLT1 Studied by Tryptophan Scanning and Affinity Labeling, *J. Biol. Chem. 278*, 49154−49163) and alkyl glucosides (Raja, M. M., Kipp, H., and Kinne, R. K. H. (2004) C-Terminus Loop 13 of Na^+ Glucose Cotransporter SGLT1 Contains a Binding Site for Alkyl Glucosides, *Biochemistry 43*, 10944−10951). Topology of this loop with regard to the membrane lipids is hitherto a point of debate. Here we report on in vitro incorporation studies using fluorescence of Trp mutants of loop 13 to determine the position of various parts of the loop with the lipid bilayer. Six single Trp mutants were prepared as described in previous studies (Raja et al., 2003) and subsequently incorporated into DOPC:DOPG (60:40% molar ratio) lipid vesicles. Upon addition of the phospholipids only one mutant, R601W, exhibited no change in the fluorescence intensities, position of maxima, or acrylamide accessibility. Mutants Q581W, E621W, and L630W exhibited the most pronounced blue shifts (3−6 nm) and protection against acrylamide, suggesting a position of these segments within the lipid bilayer. This assumption was confirmed by the result that the fluorescence of only these mutants was quenched by doxyl spin membrane embedded labels in the 5- or 12-positions of the acyl side chain of phospholipids. The other parts of the peptide appear to remain outside of the lipid vesicles. Trp-591 and Trp-611 showed, although to a different extent, increase in fluorescence, blue shift of maxima, and decrease in acrylamide accessibility but no interaction with the spin-labeled phospholipids. This suggests changes in the conformation of the peptide itself. These conformation changes are probably induced by the interaction of an adjacent lysine rich region of the peptide with the negatively charged DOPG, since in the absence of this lipid no incorporation of loop 13 into the bilayer is observed. Trypsin cleavage experiments of loop 13 in proteoliposomes yield a peptide containing amino acid residues 603 to 614, confirming that this part of the loop is accessible at the extravesicular face of the membranes. The studies show that at least in the in vitro system the part of loop 13 essential for the interaction with the transport inhibitors is located extracellularly, making a similar arrangement in the intact SGLT1 probable.

SGLT1[1] as a high affinity glucose transporter mediates transepithelial transport of D-glucose in the brush-border membranes of the small intestine and kidney by utilizing the electrochemical gradient of sodium (*3*). The intestinal Na^+-glucose cotransporter SGLT1 was expression-cloned in 1987, and found to be the first member of a new gene family. Information on the orientation of SGLT1 within the membrane can provide essential clues in understanding the structure−function relationship of this important cotransporter protein.

The protein consists of 662−665 amino acid residues with 14 putative transmembrane domains joined through several extracellular or intracellular loops (*3*). The topology of SGLT1 within the membrane is, however, still a matter of argument. The localization of the loop residues, particularly the large loop close to the C-terminal end (amino acid residues 541−638), called loop 13, has been placed either facing the cytosol or the extracellular space or within the membrane (*4*, *5*, *6*). Recently this loop, in particular the region between amino acid residues 601 and 611, has been identified as a functional domain containing phlorizin and alkyl glucosides binding sites (*1*, *2*).

The computer analysis is not always unequivocal; thus, a direct approach to determine the topology is preferable. Such studies have for example been performed by Breukink et al. (*10*), who studied the topology of nisin in the membrane

† This work was supported by funds of the IMPRS-CB (International Max Planck Research School in Chemical Biology).

* To whom correspondence should be addressed. Mailing address: Department of Epithelial Cell Physiology, Max Planck Institute of Molecular Physiology, Otto-Hahn-Str. 11, 44227 Dortmund, Germany. E-mail: rolf.kinne@mpi-dortmund.mpg.de. Tel: +49 (0) 231-133 2200. Fax: +49 (0) 231-133 2299.

[1] Abbreviations: DOPC, dioleoylphosphatidylcholine; doxyl-PC, synthetic 1-palmitoyl-2-stearoyl (*n*-doxyl)-*sn*-glycero-3-phosphocholine; DOPG, dioleoylphosphatidylglycerol; SGLT1, dodium-D-glucose cotransporter; SDS−PAGE, sodium dodecyl sulfate polyacrylamide gel electrophoresis; Trp, tryptophan; PBS, phosphate-buffered saline; Bis-Tris, 2-[bis(2-hydroxyethyl)amino]-2-(hydroxymethyl)propane-1,3-diol; MALDI-TOF, matrix-assisted laser desorption ionization time-of-flight.

10.1021/bi050323d CCC: $30.25
Published on Web 06/07/2005

using Trp scanning. To obtain information about the arrangement of loop 13 in the membrane, we performed incorporation of recombinant wild type and single Trp mutants of loop 13 in lipid vesicles containing negatively charged lipids. Changes in Trp fluorescence intensity and/or fluorescence maxima, quenching of Trp by membrane-embedded spin labels at the 5- and 12-positions, and protection against acrylamide in the presence of vesicles were measured. Thereby direct information about the depth of penetration of loop 13 into the membrane was obtained. Furthermore, enzymatic digestion was performed to cleave the accessible parts of the peptide by trypsin. All findings indicate that the potential inhibitor binding domains on loop 13 are located at the extravesicular face of the membranes, suggesting an extracellular orientation of this part of the SGLT1 in natural membranes.

EXPERIMENTAL PROCEDURES

Materials. DOPC, synthetic 1-palmitoyl-2-stearoyl (*n*-doxyl)-*sn*-glycero-3-phosphocholine (doxyl-PC), with the spin labels at the 5- and 12-positions of the *sn*-2 acyl chain, and DOPG were purchased from Avanti Polar Lipids Inc. The following chemical reagents were purchased from either Fluka (Neu-Ulm, Germany) or Aldrich (Steinheim, Germany) available in the highest purity: trypsin agarose, EDTA, Tris-base, glycine, NaCl, α-cyano-4-hydroxycinnamic acid and isopropyl-β-D-thiogalactopyranoside.

Site-Directed Mutagenesis. Mutagenesis experiments were performed using the Chameleon double-stranded, site-directed mutagenesis kit (Stratagene) as described previously (*1*). The mutations were the same as those used for the previous phlorizin binding studies (*1*) The recombinant plasmids were transformed into BL21 (DE3) cells for expression of 75 amino acid long mutant peptides of loop 13 of SGLT1.

Preparation of Recombinant Peptides. Amino terminal GST tag peptides of wild type and all mutants (amino acid residues 564−638) were expressed in *Escherichia coli* cells in Luria−Bertani medium supplemented with 100 μg/mL ampicillin as an antibiotic. Expression of the peptides was induced by addition of 1 mM isopropyl-β-D-thiogalactopyranoside for 3.5 h at 37 °C in a 2 L culture. Cells were pelleted by centrifugation at 8000 rpm for 10 min at 4 °C and resuspended in 20 mL of PBS lysis buffer [140 mM NaCl, 2.7 mM KCl, 10 mM Na_2HPO_4 and 1.8 mM KH_2PO_4 (adjusted to pH 7.4)] supplemented with 5 mM DTT, 0.1% Triton X-100, 1 mg/mL lysozyme, and protease inhibitor cocktail (one tablet). Cells were effectively lysed using a SONOPULS ultrasonic homogenization system under mild conditions. The lysate was centrifuged at 17 000 rpm for 45 min at 4 °C. The supernatants containing GST tag peptides were applied to glutathione-Sepharose columns (Amersham Biosciences, Freiburg, Germany) after being passed through a 0.2 μm filter. Soluble fractions of all peptides after removal of the protease inhibitor were generated by treating the glutathione-sepharose-immobilized fusion peptide, derived from pGEX-4T-1, with 2 units/mL of thrombin in PBS (pH 7.4) for 16 h at 4 °C. The purity of the peptides was at least 90% as assessed by SDS−PAGE using a precast Bis-Tris 4−12% gel in Tris-glycine running buffer and staining with Coomassie Blue. All peptide concentrations were determined by the method of Lowry using bovine serum albumin as a standard (*7*).

Incorporation of Isolated Peptides. Phospholipids were mixed in desired ratios in chloroform solution and dried under argon gas. Next, the lipid film was slowly (1−2 h) hydrated at a final concentration of 10 mg/mL by incubation at room temperature in PBS (pH 7.4). Small unilamellar vesicles were prepared by sonication according to the manufacturer's instructions. A homogeneous liposome size distribution of ∼75 nm was confirmed by dynamic light scattering analysis, using a dynamic light scattering ISS720 device. Vesicles were freshly prepared for all incorporation studies. After mixing 3 μM of each peptide with total lipid concentration of 150 μM, the reaction mixture was incubated at room temperature for 10−20 min prior to collecting the pellet.

Determination of Peptide to Lipid Ratio. Proteoliposomes were collected by centrifugation at 100,000*g* at 4 °C for 30 min, followed by washing 2 times with washing buffer (300 mM NaCl, 2.7 mM KCl, 10 mM Na_2HPO_4, and 1.8 mM KH_2PO_4 (adjusted to pH 7.4). Proteoliposomes were analyzed for the amount of incorporated peptide by SDS−PAGE using a precast Bis-Tris 4−12% gel in Tris-glycine running buffer stained with Coomassie Blue and by determining the protein concentration by the Lowry method after precipitating protein with 10% trichloroacetic acid.

Trp Fluorescence Measurements. All fluorescence experiments were performed in 300 μL of PBS (pH 7.4) using a Perkin-Elmer LS 50B fluorescence spectrometer (Perkin-Elmer), fitted with a 450 W xenon arc lamp at room temperature. A 0.3 cm excitation and emission path length quartz cell was used for all of the fluorescence measurements. The excitation wavelength was set at 295 nm for selective excitation of Trp. Emission spectra were collected from 300 to 400 nm, averaging six scans. The bandwidths for both excitation and emission monochromators were 5 nm. The emission spectra were corrected (1) for the vesicle blank (scatter) which at the maximal lipid concentration used contributed at most 25% to the total signal, (2) for dilution effects, and (3) for the inner-filter effect.

Doxyl-Labeled Lipid Quenching Experiments. To examine the depth of the Trp residues of the different loop 13 mutants in the membrane bilayer, vesicles were prepared containing 10% doxyl-PC. The change of fluorescence intensity upon addition of 150 μM lipid vesicles containing 10% doxyl-PC to a solution of 3 μM loop 13 mutants (F) was compared to the fluorescence intensity change upon addition of the same amount of vesicles containing unlabeled PC (F_0). The data were analyzed as quenching efficiencies, according to

$$\text{quenching efficiency} = (1 - F/F_0) \times 100\%$$

The differences in quenching of the Trp fluorescence depending on the position of the spin label were used to determine the most probable location of Trp in the membrane as developed by Chung et al. (*8*).

Acrylamide Quenching Experiments. Acrylamide quenching experiments were carried out in PBS (pH 7.4) at an excitation wavelength of 295 nm to reduce the absorbance by acrylamide. Small aliquots of acrylamide were added from 5.0 M stock solution to 3 μM of each peptide solution up to

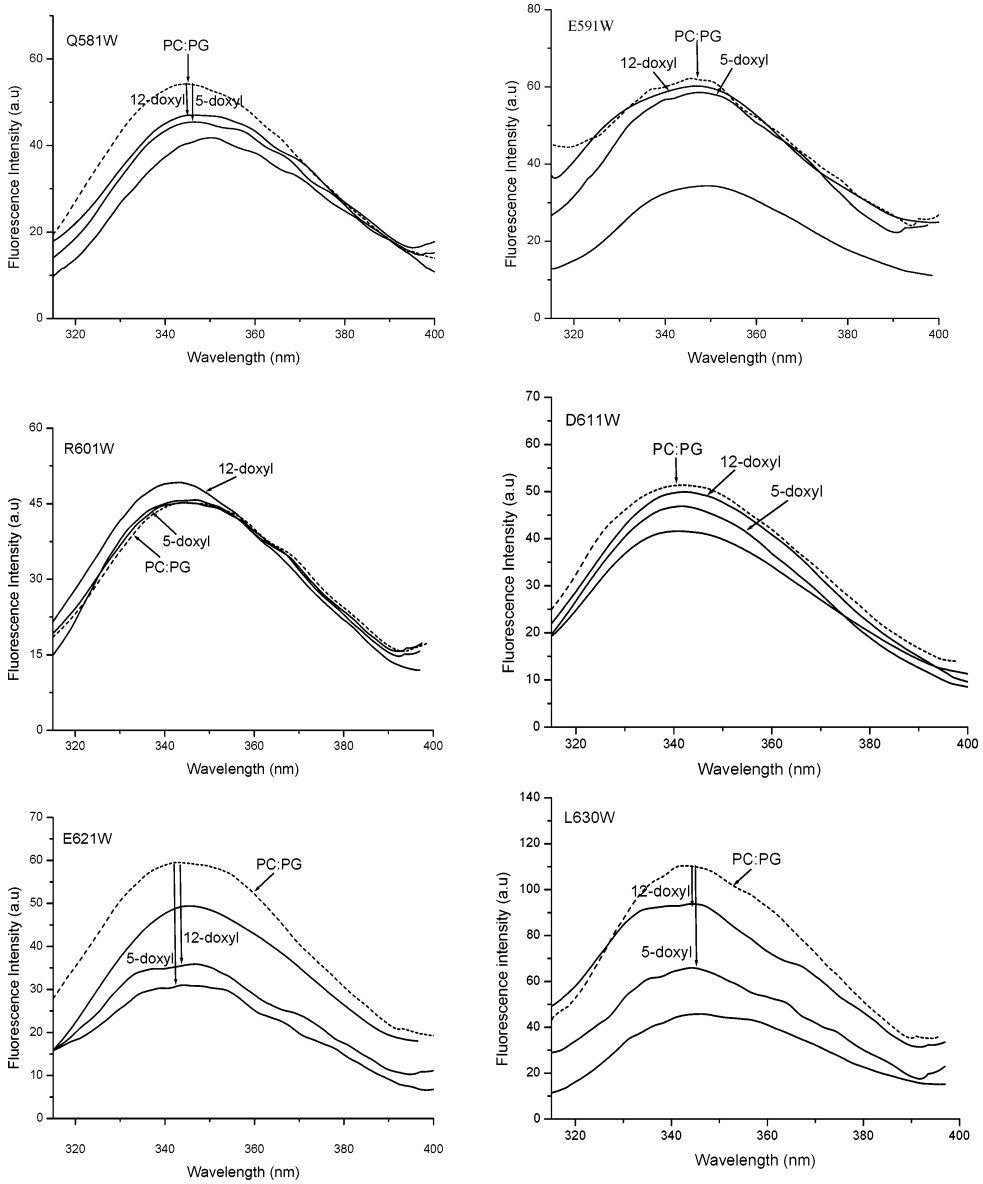

FIGURE 1: Effect of DOPC:DOPG (60:40%) on fluorescence emission spectra of single Trp mutants of loop 13. The solid lines show the corrected spectra of Trp mutants (3 μM) in simple buffer (PBS, pH 7.4). Vesicles composed of 60% PC, 40% PG (dotted lines) or 50% PC, 40% PG, 10% doxyl-PC labeled at either the 5- or the 12-position of the *sn*-2 acyl chain were prepared and mixed with mutant peptides (3 μM) in PBS, pH 7.4. All of the spectra were corrected as described in Experimental Procedures; a.u., arbitrary units.

350 mM in the absence or in the presence of 150 μM lipid vesicles.

The data were analyzed according to the Stern−Volmer equation (*9*),

$$F_0/F = 1 + K_{SV}[Q]$$

where F_0 is the fluorescence of the peptide in the absence of quencher and F is the observed fluorescence at the concentration of the quencher ([Q]). K_{SV} is the collisional quenching constant which was determined from the slope of best fit values of Stern−Volmer plots at a given concentration of the quencher.

Trypsin Digestion of Incorporated Peptide. A part of proteoliposome's pellet of wild type loop 13 incorporated in lipid vesicles was resuspended in 300 μL of PBS (pH 7.4), and 50 μL of trypsin beads on agarose basis (50% slurry) was added to proteoliposomes. The mixture was allowed to incubate in an Eppendorf tube at room temperature for 4 h with gentle rotation. Proteoliposomes were collected by centrifugation, and supernatant was concentrated to a small volume using an ultramicrofilter with a cutoff of 0.1 kD. The peptides were then precipitated by the chloroform−methanol method and dried in a centrifugal evaporator. The peptide pellet was dissolved in a small volume of 50% acetonitrile plus 0.1% trifluoroacetic acid. An aliquot of 0.5 μL of cleavage product was placed onto the sample support, followed by 0.5 μL of α-cyano-4-hydroxycinnamic acid matrix solution (solution of α-cyano-4-hydroxycinnamic acid in 0.1% trifluoroacetic acid in 50% acetonitrile). Samples were deposited on a MALDI plate and dried at room temperature prior to collection of the spectra.

RESULTS

Effect of Lipid Vesicles on Trp Fluorescence. The corrected Trp fluorescence spectra (λ_{exc} = 295 nm) of Q581W, E591W, R601W, D611W, E621W, and L630W in the absence and presence of 150 μM PC:PG (60:40%) are shown in Figure

Table 1: Effect of Vesicles on Trp Fluorescence of Single Trp Mutants[a]

peptide	fluorescence intensity (%) (increase)[b]	fluorescence maxima (nm)		
		no vesicles	PC:PG (60:40%)	Δ[c] (shift)
Q581W	23	348	342	−6
E591W	28	349	347	−2
R601W	0	342	342	0
D611W	20	341	340	−1
E621W	17	343	340	−3
L630W	60	343	340	−3

[a] The data were derived from Figure 1. [b] The values are the percentage of increase in fluorescence in the presence of PC:PG (60:40%). [c] Δ represents the differences between the values. A minus sign indicates a blue shift in maxima.

Table 2: Fluorescence Quenching by Membrane-Embedded Doxyl Spin Labels[a]

Trp mutants	% quenching	
	5-doxyl spin label	12-doxyl spin label
Q581W	14	12
E591W	4	2
R601W	1	−4
D611W	9	3
E621W	50	41
L630W	38	14

[a] All spectra from Figure 1 were integrated and normalized relative to the fluorescence obtained using lipid vesicles consisting of PC:PG (60:40%) lacking the doxyl spin label. The percent quenching, relative to the total increase in fluorescence in the presence of PC:PG (60:40%) without nitroxide spin labels, is listed.

1 and compiled in Table 1. Increase in fluorescence and shifts in the maximum to shorter wavelengths were observed for all mutants, although to a different extent, except for R601W, which exhibited no change.

Fluorescence Quenching by Membrane-Embedded Doxyl Spin Labels. The liposome-induced blue shifts and increases in fluorescence intensity of Trp mutants suggest that, upon formation of the peptide−lipid complex, the Trp residues Q581W, E591W, E621W, and L630W shift to a more hydrophobic environment. This relatively hydrophobic environment could lie either within the protein or in the lipid bilayer. To discriminate between these possibilities, we examined the ability of lipid-embedded nitroxide spin labels to quench the fluorescence of each Trp reporter group. Only Trp residues that can interact directly with the nitroxide spin groups become quenched. For these experiments, PC:PG (60:40%) vesicles were prepared that contained doxyl-PC labeled at either the 5- or the 12-position of the *sn*-2 acyl chain.

All Trp mutants were mixed with a constant amount of vesicles containing 50% PC, 10% doxyl-PC, and 40% PG. The spectra from these experiments are shown in Figure 1, and the degree of quenching by the nitroxide groups is tabulated in Table 2. From these spectra, it is apparent that the doxyl spin labels efficiently quenched Trp-621 and -630. Trp fluorescence of E621W is strongly quenched by the 5-doxyl spin label, and the 12-doxyl spin label has almost the same effect. This would suggest a deep embedding of Trp-621 in the membrane. L630W fluorescence is also strongly quenched by the 5-doxyl but less quenched by the 12-doxyl spin label. This finding would be explained by the assumption that Trp-630 enters the second monolayer and resides close to the 5-doxyl spin label of the second monolayer. This deep positioning also explains the maximum increase in Trp fluorescence.

The fluorescence of other mutants was not directly quenched by doxyl spin labels. Comparatively less quenching of an increased fluorescence induced by PC:PG (60:40%) vesicles was observed for Q581W and D611W by doxyl spin labels. In addition, no change was observed for R601W.

Effect of Lipid Vesicles on Trp Accessibility to Collisional Quenching. The calculated blue shifts of Trp mutants and quenching by membrane-embedded spin-labeled PC vesicles suggested that some parts of loop 13 might be embedded within the lipid bilayer. This was assessed in a more direct manner by means of acrylamide, a hydrophilic quencher of the Trp fluorescence. In addition, this quencher has the advantage that it has a very low permeability to lipid membranes.

The Stern−Volmer quenching plots of each mutant in the absence and presence of phospholipid vesicles consisting of PC:PG (60:40%) were linear and are shown in Figure 2. The Stern−Volmer constants for all mutants are compiled in Table 3. It indicates that the Trp residues are more or less protected against quenching by acrylamide. As expected, Trp-621 and Trp-630 are completely protected. This supports their location in the lipid environment. Surprisingly, Trp-591 despite no interaction with the nitroxide quencher shows strong protection, suggesting an effect of lipid vesicles on folding of the peptide chain. Slight changes are also observed for Trp-581 and Trp-611; Trp-601 appears not to be affected.

Effect of Lipid Composition on Trp Accessibility to Collisional Quenching. In addition, the calculated quenching constants of each Trp accessibility in the absence and presence of 150 μM pure PC and PC:PG (70:30%) are shown in Table 4 (plots are not shown). The data shows that K_{SV} values for all mutants in the presence of pure PC and PC:PG (70:30%) are significantly lower compared to the K_{SV} values in the presence of PC:PG (60:40%) vesicles. Thus, the negatively charged PG seems to favor the interaction and/or the orientation of loop 13 mutants with and/or within the membranes (see Discussion).

MALDI Mass Spectrometry of Incorporated Loop 13 in Lipid Vesicles. To identify which parts of loop 13 are located outside of the vesicles consisting of PC:PG (60:40%), proteoliposomes of incorporated wild type loop 13 were subjected to trypsin digestion. After collecting the supernatant and precipitating the cleavage products, the resulting mixture was analyzed in the MALDI-TOF mode. As a control, a sample was prepared with the same procedure except that it did not contain loop 13. The only additional peak observed in an experimental probe was at *m*/*z* 1387.23 (Figure 3), which corresponds to a 12 amino acid long peptide from alanine-603 to lysine-614 of loop 13 [for more detail see previous studies (*1*)]. All other peaks appeared also in the control (not shown). These data confirm that this part of loop 13 resides outside the membrane.

DISCUSSION

In this study we performed incorporation of wild type and six single Trp mutants of loop 13 to elucidate the localization of various parts of loop 13 at the extravesicular face or within

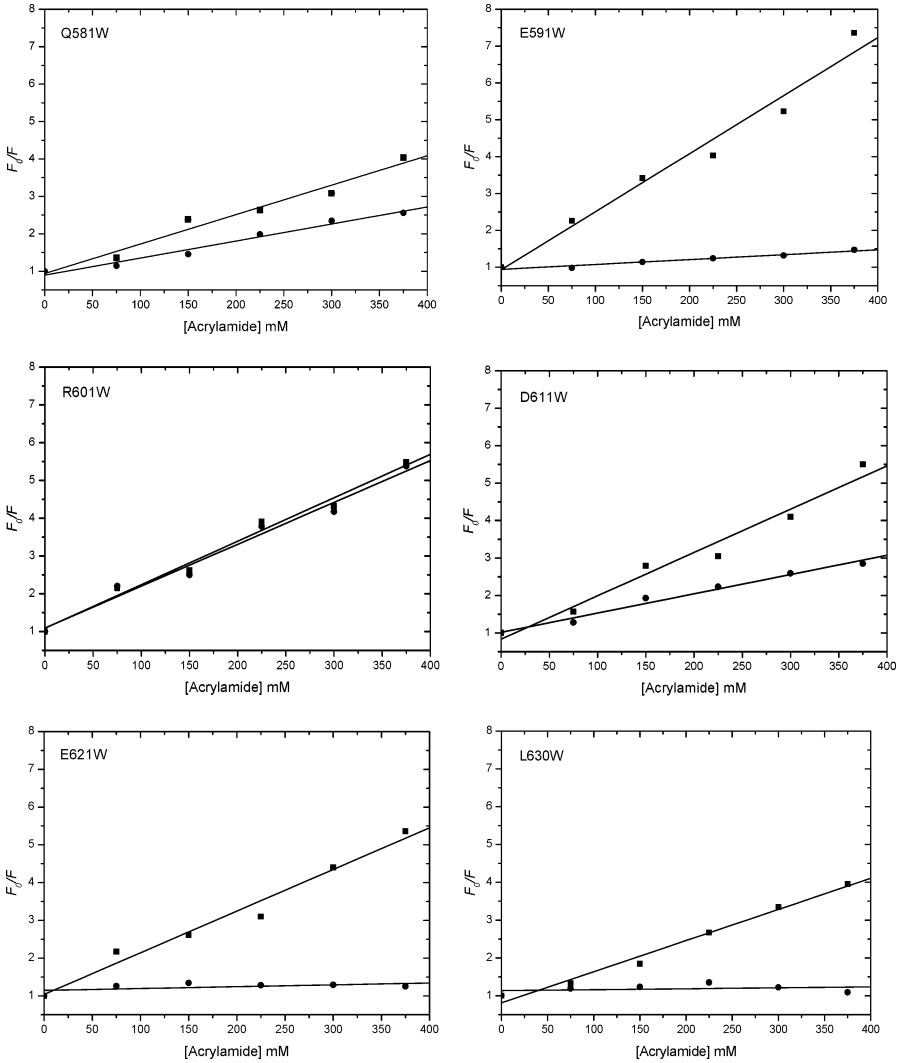

FIGURE 2: Stern−Volmer plots of Trp fluorescence quenching by acrylamide. Quenching experiments were conducted as described in Experimental Procedures. In each panel the samples were investigated in the absence (■) and presence of (●) 150 μM PC:PG (60:40% molar ratios). The slopes of the best fit lines for each data set (K_{SV} values) are shown in Table 3. Mean values ± standard deviation of two or three independent experiments are given.

Table 3: Stern−Volmer Constants of the Effect of PC:PG (60:40%) on Single Trp Mutants of Loop 13[a]

peptide	DOPC:DOPG (60:40%)[b]	K_{SV}[c] (M^{-1})	peptide	DOPC:DOPG (60:40%)[b]	K_{SV}[c] (M^{-1})
Q581W	−	7.4	D611W	−	8.8
	+	4.5		+	5.4
E591W	−	15.2	E621W	−	10.6
	+	2.5		+	1
R601W	−	11.1	L630W	−	8.4
	+	10.6		+	1

[a] Parameters of acrylamide accessibility were derived from the data shown in Figure 2. [b] Quenching experiments were conducted in the absence (−) or presence (+) of 150 μM PC:PG (60:40%). [c] The Stern−Volmer constants were determined from the slopes of the linear regression lines from plots of $F_0/F = 1 + K_{SV}[Q]$. Values are mean ± standard deviation of two or three independent experiments.

Table 4: Influence of Lipid Composition of Vesicles on the Trp Fluorescence of Loop 13 Mutants[a]

peptide	no lipid[b]	DOPC[b,c]	DOPC:DOPG (70:30%)[b,c]
Q581W	7.4	6.6	-
E591W	15.2	11.8	7.3
R601W	11.1	13.4	11.4
D611W	8.8	8.2	6.1
E621W	10.6	11.0	1.5
L630W	8.4	7.8	1.9

[a] Stern−Volmer constants (M^{-1}) for 3 μM of each Trp mutant in the absence and presence of vesicles (150 μM) of various compositions. [b] The Stern−Volmer constants were determined from the slopes of the linear regression lines from plots of $F_0/F = 1 + K_{SV}[Q]$. Values are mean ± standard deviation of two or three independent experiments. [c] Parameters were derived from acrylamide quenching data (not shown).

a lipid bilayer. For all mutants except 601, an increase in Trp fluorescence and blue shift in maximum was observed upon addition of negatively charged lipids which indicates the transfer of Trp residues from an aqueous to a hydrophobic environment (*10*, *11*). The changes in the fluorescence observed for the various mutants after association with lipid vesicles are summarized in Table 5. Interestingly these changes were not observed when pure PC vesicles were used. Since loop 13 contains several positively charged amino acids, an interaction with the negatively charged headgroups of PG appears to be necessary for the association of the peptide to the lipids. The findings that in the presence of 30% PG less protection of each single Trp against acrylamide

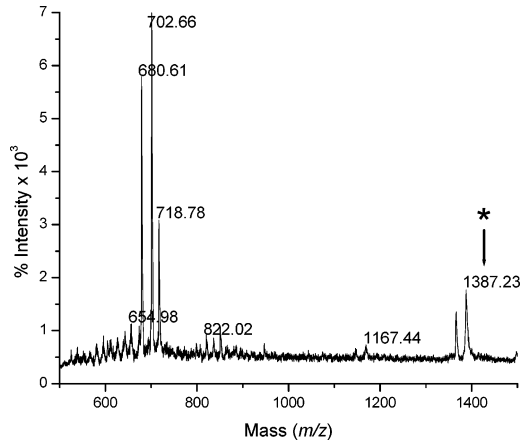

FIGURE 3: MALDI mass spectrum of trypsin digested incorporated wild type loop 13. Incorporation experiments were carried out for 3 μM wild type loop 13 in 150 μM PC:PG (60:40%). Trypsin digestion was performed and the MALDI mass spectrum was recorded as described in Experimental Procedures. The asterisk denotes the additional peak which corresponds to a small peptide (603−614 amino acid residues) [for more detail see previous studies (*1*)].

was observed than in the presence of 40% PG are consistent with this assumption.

As another major change, blue shifts in the maxima were observed. These indicate the positioning of the Trp into a more hydrophobic environment. In the experimental system employed here, this effect might be caused by insertion into the acyl side chains of the lipid phase of the phospholipids or due to a change in peptide conformation or both. We tested for the insertion into the lipid phase by employing doxyl labeled phospholipids, and we now compare the two parameters.

For Q581W, we observed a very strong blue shift in the maximum and slight fluorescence quenching by doxyl groups. It thus can be assumed that this residue resides in the bilayer (see model in Figure 4). The significant protection against acrylamide in the presence of lipid vesicles also points in this direction. The discrepancy between the large change in the spectral maximum and the relative moderate effect of the doxyl quenchers can be explained by the fact that in the absence of the lipids Trp-581 resides in a very hydrophilic environment. The insertion into the hydrophobic acyl side chains of phospholipids therefore causes the large blue shift.

E591W exhibits only a small blue shift, no quenching by doxyl derivations, and maximum protection against acrylamide upon addition of lipid vesicles. Conformational changes of the peptide, such as positioning of one helix of the peptide above Trp-591, could result in a blue shift and maximum protection of this Trp against acrylamide.

Surprisingly, no significant change in parameters of Trp fluorescence was observed for R601W in the presence of vesicles; thus, this part of the peptide appears not be involved

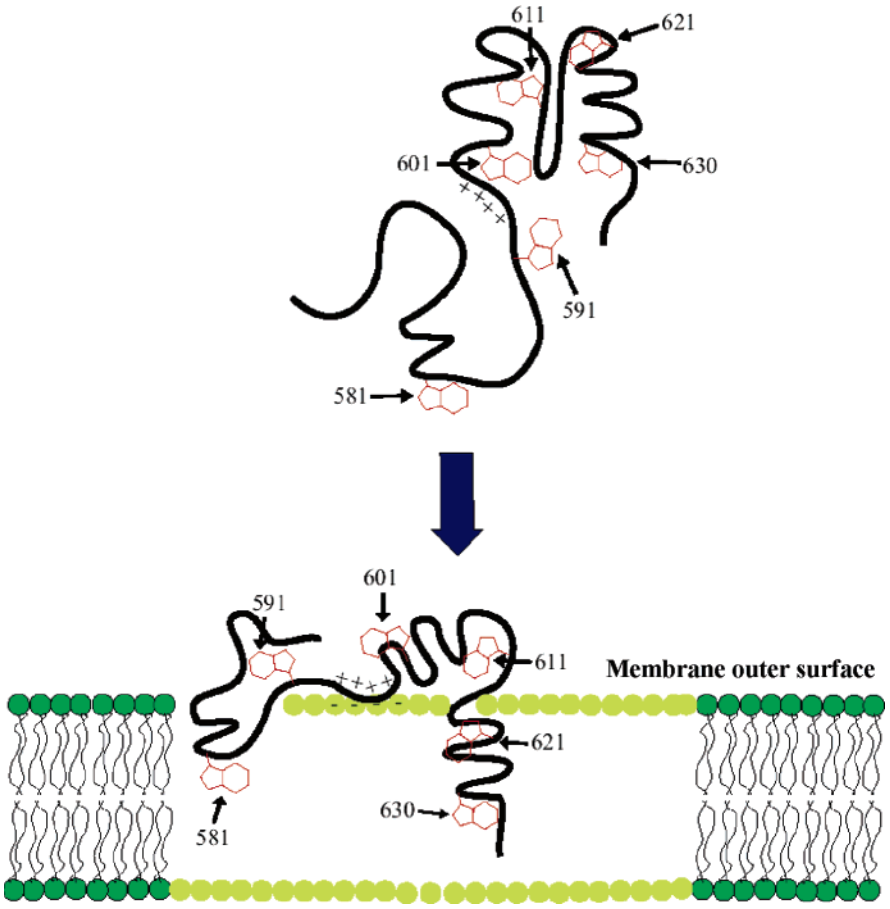

FIGURE 4: Proposed two-dimensional model of the organization of Trp residues of loop 13 in lipid vesicles. Trp residues at different positions are shown in red as aromatic rings with an indol side chain. Upper panel: An assumed conformation of the peptide as depicted (*1*) in solution. Lower panel: Conformation of the peptide assumed with Trp residues (red) in the lipid bilayer as suggested by the changes in Trp fluorescence parameters. The depth of penetration of Trp residues in membrane was determined as described by Chung et al. (*8*). The poly-lysine region is also shown in the form of positive charges.

Table 5: Effect of Lipid Vesicles on Trp Fluorescence Parameters of Loop 13 Mutants

peptide	fluorescence	blue shifts in maxima	spin label proximity	acrylamide accessibility	positioning in bilayer
Q581W	increase	very strong shift	low	decrease	yes
E591W	increase	slight shift	none	maximum decrease	no
R601W	no change	no change	none	no change	no
D611W	increase	slight shift	low	decrease	no
E621W	increase	strong shift	present	complete decrease	yes
L630W	maximum increase	strong shift	present	complete decrease	yes

in interaction with the membrane. The positively charged poly lysine residues from position 594 to 597 strongly interact with the negatively charged polar headgroups of the phospholipids, which form a major attachment site of the peptide. Studies performed by atomic force microscopy on lipid−peptide interaction suggest a similar situation (Wimmer et al., unpublished data; see also model in Figure 4).

For positions 621 and 630 the strong blue shift in maxima and the quenching by doxyl labels strongly suggest immersion of this region into the acyl side chains of the phospholipids. The position of Trp-621 is probably closer to the center of the lipid bilayer than that of Trp-630 because the doxyl labels at C5 and C12 quench the Trp fluorescence to the same extent in 621 whereas the effect of the label at C5 is stronger for Trp 630 (see model in Figure 4). This conclusion is also supported by the facts that both Trp residues become completely inaccessible to acrylamide and that this part of the peptide is also predicted to form a short hydrophobic α-helix. The insertion of the loop pulls 611 close to the membrane as evidenced by the decreased accessibility to acrylamide.

To further characterize the orientation of loop 13 in the proteoliposomes, we performed trypsin digestion where only peptide segments present extravesicularly are attacked. A detectable cleavage product directly proves that amino acid residues 603−614 reside extracellularly. This observation is also consistent with our Trp fluorescence studies.

The topology of loop 13 in artificial membranes cannot assign the position of the early part of loop 13 (e.g., amino acid residues 564−580) studied here since no experimental data are available. However, the early parts of loop 13 also contain phosphorylation motifs for protein kinases at the 562 position (*12*) that in order to be physiologically relevant in the intact cells have to be exposed to the cytoplasm. A verification of the extramembranous orientation of the late part of loop 13 (amino acid residues 606−630) was obtained by Wielert-Badt et al. (*13*) using molecular recognition atomic force microscopy on isolated natural membrane vesicles. In addition to these studies, the current findings are also consistent with the extracellular location of loop 13 which strongly reacts with an antibody, raised against amino acid residues 606−630, from outside of intact cells (*6*).

In fact it is difficult to compare the conformation of isolated loop 13 studied here with the whole protein in intact carrier. However, the topology of loop 13 in the membrane is consistent with the observations of in vitro as well as in vivo studies where phlorizin and alkyl glucosides interact with the hydrophobic parts of the transporter which were found on loop 13 (*1*, *2*, *14*, *15*). The regions 600 to 611 (a phlorizin binding pocket) and 601 to 619 which contain binding sites for alkyl glucosides should be located extracellularly to provide interaction sites on SGLT1 as is suggested by our studies.

ACKNOWLEDGMENT

The authors like to gratitude Prof. Dr. Roland Winter for his helpful suggestions on experimental work. The careful secretarial work of Natascha Kist-Gruel and experimental help of Kirsten Michel are gratefully acknowledged.

REFERENCES

1. Raja, M. M., Tyagi, N. K., and Kinne, R. K. H. (2003) Phlorizin Recognition in a C-terminal Fragment of SGLT1 Studied by Tryptophan Scanning and Affinity Labeling, *J. Biol. Chem. 278*, 49154−49163.
2. Raja, M. M., Kipp, H., and Kinne, R. K. H. (2004) C-Terminus Loop 13 of Na^+ Glucose Cotransporter SGLT1 Contains a Binding Site for Alkyl Glucosides, *Biochemistry 43*, 10944−10951.
3. Wright, E. M. (1993) The intestinal Na^+/glucose cotransporter, *Annu. Rev. Physiol. 55*, 575−589.
4. Turk, E., Martn, M. G., and Wright, E. (1994) Structure of the human Na+/glucose cotransporter gene *SGLT1*, *J. Biol. Chem. 269*, 15204−15209.
5. Turk, E., Kerner, C. J., Lostao, M. P., and Wright, E. M. (1996) Membrane topology of the human Na+/glucose cotransporter SGLT1, *J. Biol. Chem. 271*, 1925−1934.
6. Lin, J. T., Kormanec, J., Homerova, D., and Kinne, R. K. H. (1999) Probing Transmembrane Topology of the High-Affinity Sodium/Glucose Cotransporter (SGLT1) with Histidine-Tagged Mutants, *J. Membr. Biol. 170*, 243−252.
7. Lowry, O. H., Rosebrough, N. J., Farr, A. L., and Randall, R. J. (1951) Protein measurement with the folin phenol reagent, *J. Biol. Chem. 193*, 265−275.
8. Chung L. A., Lear J. D., and DeGrado W. F. (1992) Fluorescence studies of the secondary structure and orientation of a model ion channel peptide in phospholipid vesicles. *Biochemistry 31*, 6608−6616.
9. Lackowicz, J. R. (1999) *Principles of Fluorescence Spectroscopy*, Kluwer Academic/Plenum, New York.
10. Breukink, E., Kraaij, C. V., Dalen, A. V., Demel, R. A., Siezen, R. J., Kruijff, B. D., and Kuipers, O. P. (1998) The Orientation of Nisin in Membranes, *Biochemistry 37*, 8153−8162.
11. Macek, P., Zecchini, M., Pederzolli, C., Serra, M. D., and Menestrina, G. (1995) Intrinsic Tryptophan Fluorescence of Equinatoxin II, a Pore-Forming Polypeptide from the Sea Anemone *Actinia Equina* L, Monitors its Interaction with Lipid Membranes, *Eur. J. Biochem. 234*, 329−335.
12. Hediger, M. A., Coady, M. J., Ikeda, T. S. and Wright, E. M. (1987) Expression cloning and cDNA sequencing of the Na^+/glucose cotransporter, *Nature 330*, 379−381.
13. Wielert-Badt, S., Hinterdorfer, P., Gruber, H. J., Lin, J. T., Badt, D., Wimmer, B., Schindler, H., and Kinne, R. K. H. (2002) Single Molecule Recognition of Protein Binding Epitopes in Brush Border Membranes by Force Microscopy, *Biophys. J. 82*, 2767−2774.
14. Novakova, R., Homerova, D., Kinne, R. K. H., Kinne-Saffran, E., and Lin, J. T. (2001) Identification of a region critically involved in the interaction of phlorizin with the rabbit sodium-D-glucose cotransporter SGLT1 *J. Membr. Biol. 184*, 55−60.
15. Xia, X., Lin, J. T., and Kinne, R. K. H. (2003) Binding of Phlorizin to the Isolated C-Terminal Extramembranous Loop of the Na^+/Glucose Cotransporter Assessed by Intrinsic Tryptophan Fluorescence, *Biochemistry 42*, 6115−6120.

BI050323D